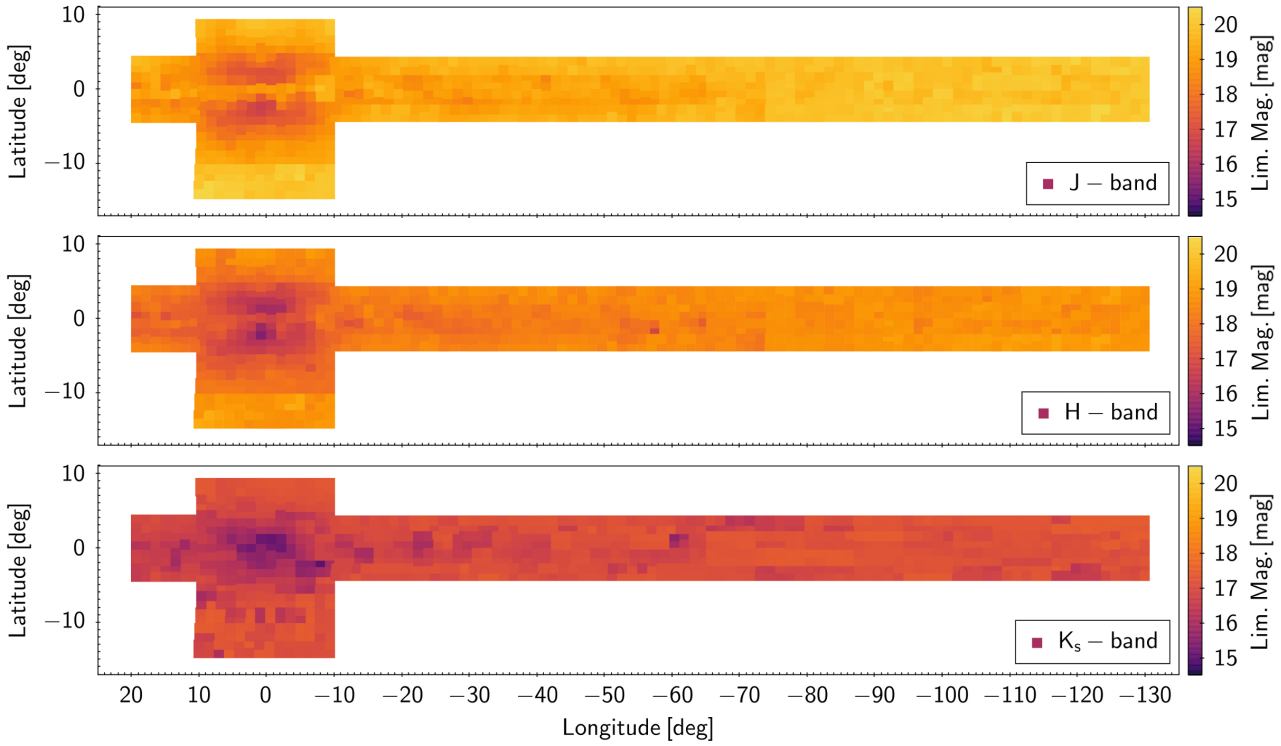

Fig. 4. 5σ magnitude limits of the catalogues in the J, H, and K_s, respectively, from top to bottom. The colour scale is the same in the three panels as shown in the vertical bars at the right. For the J and H bands, VVV and VVVX are combined because of the lack of VVVX observation in these bands in the original VVV area.

J filter only OBs were observed in order to double the exposure time in that filter. The deep J imaging corresponds to a time on source of ∼4 min, and due to the 1 h restriction on OB duration, these additional J filter observations had to be separate from the JHK_s observations, for a given tile. The two J images for each tile can be coadded to increase the useful depth of K_s vs. $J - K_s$ colour magnitude diagrams. For instance, the combined K_s epochs and the deep J will reach $J = 20.8$ mag, $K_s = 20$ mag at 5σ, which is three magnitudes fainter than the unreddened bulge main-sequence turnoff. The densest fields will be confusion-limited, but applying both point-spread function (PSF) fitting techniques and differential photometry (DIA), it is possible to recover most objects down to $J = 19.5$ mag, $H = 18.5$ mag and $K_s = 18$ mag, even in fairly crowded fields. This is more than 3 mag fainter than the unreddened RR Lyrae in the Galactic bulge.

Contemporaneous JHK_s epochs give the colours for variable stars (essential for precise dereddening of RR Lyrae and Cepheids) while the deep J observations allow the construction of deep colour-magnitude diagrams reaching past the age-sensitive main sequence turn-off. Because denser fields are confusion-limited, the limiting magnitudes vary along the area, especially in the innermost bulge area. Figure 4 shows the limiting magnitudes as a function of position for all the filters.

The J and H observations were ≳85% and ≳95% complete by the end of the 2018 and 2019 season, respectively. The median image quality in J and H are 0.88″ and 0.84″ for a median airmass of 1.19 and 1.17, respectively, measured on combined tile images (see Fig. 5). The image quality is measured from the average FWHM of sources classified as bona fide stars with high signal-to-noise. This value includes atmospheric, telescope and instrument related aberrations and is not the same as seeing, which is an inherent property of the atmosphere independent of the telescope (Martinez et al. 2010). We refer to Sutherland et al. (2015) for a detailed description of the image quality design and performance of the VIRCAM@VISTA. In K_s, the observations exceeded ≳90% completeness only in 2022, with median image quality of 0.93″ for a median airmass of 1.21. In most cases the observations satisfied the atmospheric turbulence and photometric image quality parameters and were classified as completed. Remaining JH observations were taken during 2020–2022 and K_s in 2020–2023 to complete the planned observations within the photometric and image quality parameters.

We summarise in Table 3 the observed areas along the years of the VVVX campaign. Regarding the multicolour data, the JHK_s observations were ≳94% complete by the end of the 2019 season. The remaining observations were secured during 2020–2023 and comprised repeated observations of the tiles that did not pass the quality control in the first instance. The cumulative distributions for the JHK_s are presented in Fig. 6.

The VVVX observations were pipeline-processed at the Cambridge Astronomical Survey Unit (CASU), using the VISTA data flow system (VDFS) pipeline (Lewis et al. 2010). CASU also produces the photometric calibration of stacked pawprint images and tile images (González-Fernández et al. 2018). Multiband catalogues have also been generated by the VISTA Science Archive (VSA). All tiles, their confidence maps and extracted source lists, in addition to the corresponding pawprints, were processed with version 1.5 of the CASU pipeline. In the catalogues provided by CASU, a flag is used to indicate the most probable morphological classification. These flags were derived from the curve-of-growth analysis of the flux from different aperture sizes (Irwin et al. 2004). The flags are:

- '−1' to denote stellar objects,
- '−2' to denote borderline stellar,
- '−7' denoting sources containing bad pixels,

Table 3. Summary of the VVVX observational campaign.

Area name	Area (deg^2)	No. of Tiles	RA Range (h)	2016	2017	2018	2019	2020	2021	2022	2023
VVV bulge	313	196	17h−19h	K_s	K_s	JHK_s	JK_s	–	K_s	K_s	–
VVV disk	232	152	12h−19h	K_s	K_s	K_s	K_s	–	–	K_s	–
Disk Long. +20	90	56	18h−19h	K_s	JHK_s	K_s	K_s	–	–	K_s	–
Disk Long. +230	292	180	07h−12h	–	–	JHK_s	K_s	K_s	K_s	K_s	K_s
Low Ext. Bulge	90	56	18h−19h	JHK_s	–	K_s	K_s	–	–	–	–
High Ext. Bulge	90	56	17h−18h	K_s	JHK_s	K_s	K_s	–	–	K_s	–
Low Ext. Disk	266	166	07h−18h	K_s	JHK_s	JHK_s	JHK_s	K_s	K_s	K_s	K_s
High Ext. Disk	266	166	07h−17h	K_s	JHK_s	JHK_s	JHK_s	K_s	K_s	K_s	K_s

Notes. J and H observations were 97% and 94% completed by the end of 2019 season. The remaining observations were taken from 2020 to 2023, mostly repeated observations. The K_s band was ≳99% completed by the end of the 2022 season. Only residual K_s observations, comprising ≲1% of the total, were taken in year 2023 to complete the planned observations.

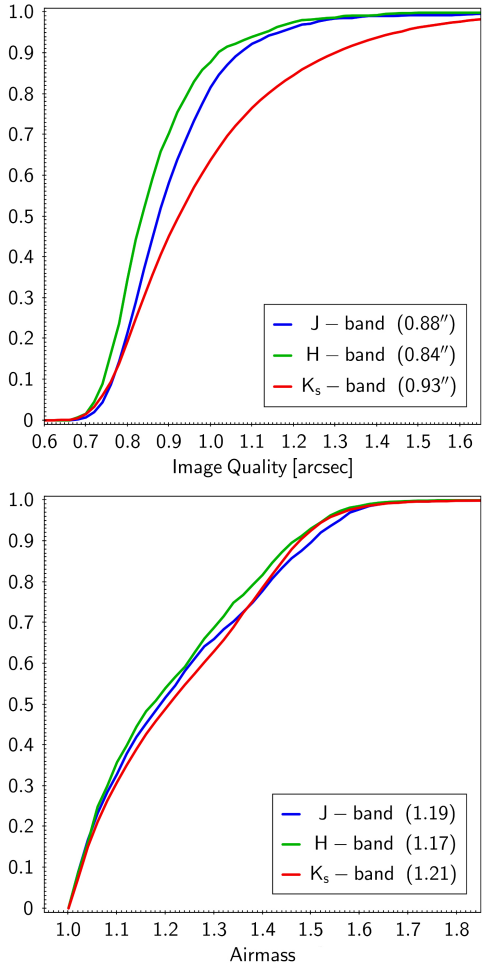

Fig. 5. Image quality and airmass cumulative distributions for the JHK_s VVVX observations, in the top and bottom panels, respectively. The median values of image quality and airmass for each filter are presented in the legends.

- '−9' is used for saturated stars,
- '+1' is used for non-stellar objects and
- '0' is used to denote a noise measurement.

The entire reduction and calibration process is same as that applied to the VVV data. For more details on data processing and catalogue generation, we refer the reader to Sects. 2 and 3 of the VVV DR1 paper (Saito et al. 2012) and the references therein.

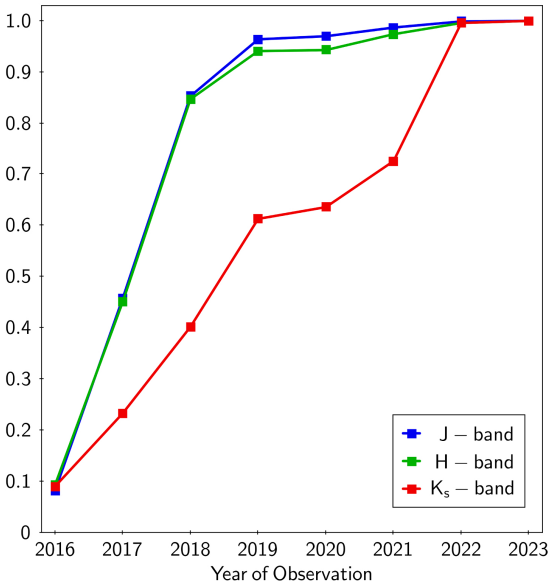

Fig. 6. Cumulative distributions for the JHK_s observations during the VVVX campaign.

5. Previous data releases

The first VVVX data release (VVVX DR1[6]) was published in February 2019 and contains data acquired between July 2016 and August 2017. The first release contains observations of about 590 sq. deg., typically covered in the three filters (J, H and K_s). DR1 released a total of 1660 tile images that passed quality control, plus their associated weight maps and single-band source catalogues. Moreover, it contains 9960 pawprint images and their associated weight maps that were used to create the tile images. The total data volume is about 1.7 TB in compressed format (CFITSIO RICE compression[7]).

[6] https://www.eso.org/rm/api/v1/public/releaseDescriptions/130
[7] http://wsa.roe.ac.uk//qa.html#compress

In June 2021, we publicly released the VVVX DR2[8] with the data taken between April 2018 and October 2019. They consist of both multicolour JHK_s observations and K_s band variability data. The DR2 has 10776 tile images, plus their associated single-band source catalogues and weight maps. For the pawprints, there is a total of 64 716 images, plus the single-band source catalogues and weight maps. The total data volume is eight times larger than DR1, reaching 13.4 TB in compressed format. The uncompressed data volume of the VVVX DR1 plus VVVX DR2 is $\gtrsim$27 TB.

The K_s band taken prior to April 2018 was not released with the VVVX DR1, which contained data only from the multicolour JHK_s OBs and J-only OBs. JHK_s and J-only OBs taken during 2020–2022, as well as K_s from 2020 to 2023, represent a smaller part of the total volume. These data had been gradually processed by CASU and VSA, and ingested to the ESO Archive, with no announcement of a public data release. These remaining data complete the release to the astronomical community of all the observations planned by VVVX within the established quality criteria. In total, the VVV+VVVX survey observations comprise >350 000 images, which including images, catalogs and confidence maps, they make a total of more than 10^6 files.

The VVVX data, as described above, can be downloaded directly via the ESO Archive[9]. Various options are available for how the data can be obtained, from simple cone searches to more complex options. In the ESO Archive it is also possible to browse the VVVX data using an Aladin Sky Atlas tool, and by clicking and selecting, determine which data among images and catalogues are of interest for direct download.

6. Advanced data products

The images and catalogues described in the section above, already available via the VSA and ESO Archive, are being complemented by advanced products, currently under preparation by VVVX science team members. As for VVV, a key product is the extraction of PSF photometry, which is more robust and accurate than aperture photometry data for the regions of high crowding of stars, such as in the innermost MW bulge and plane, and for the study of star clusters (e.g. Alonso-García et al. 2018).

PSF-based catalogues are compiled for each VVVX tile, however measured from the stacked pawprint images, where codes such as DAOPHOT (Stetson 1987), DOPHOT (Schechter et al. 1993), and SExtractor (Bertin & Arnouts 1996) work with better precision.

As well as for the VVV Survey, various authors will provide independently produced PSF based source catalogues of the multicolour data (e.g. Alonso-García et al. 2018; Surot et al. 2019), and the variability campaign (e.g. Contreras Ramos et al. 2017; Smith et al. 2018). Specific details will be published elsewhere. The catalogues will be available through the VSA[10], using the same schema as for aperture and image data.

The K_s band variability data allows for a variety of uses, from constructing light curves to proper motion measurements. For the VVV area, our team published a number of catalogues containing hundreds of thousands candidate of variable stars, for example: the VVV Near-IR Variability Catalogue (VIVA-I; Ferreira Lopes et al. 2020), the Near-IR Catalogue of known variable stars (Herpich et al. 2021), and the VIRAC Variable Classification Ensemble (VIVACE; Molnar et al. 2022).

The extinction in K_s filter of VIRCAM is an order of magnitude lower than in optical. Hence, the VVVX proper motion data are complementary to those of *Gaia* in highly extincted Galactic disk and bulge regions, where the optical *Gaia* data result in significantly reduced depth. Over the area of the original VVV region, the K_s band data can be combined to increase the time baseline to more than a decade ($\gtrsim$2010–2020, or even 2022 for selected bulge fields), thus increasing the accuracy of the proper motion measurements. For the new extended area, the time base is approximately 4–5 yr.

Proper-motion catalogues will be incorporated into the VISTA Infrared Catalogue 2 (VIRAC2, in preparation), the latest version of the original VISTA Infrared Catalogue (VIRAC; Smith et al. 2018). Luna et al. (2023) compared the VIRAC2, *Gaia* DR3 and HST proper motions in a few fields towards the Galactic bulge, with different stellar crowding levels. The test showed that VIRAC2 proper motions have more reliable uncertainties than *Gaia* DR3 and are comparable to HST in dense fields, such as globular clusters and the Galactic bulge. The shorter time base of the new VVVX areas should influence the data quality, so we should expect larger fractional uncertainties for more distant and slower sources. VIRAC2 has been uploaded to ESO archive where it will be available for Virtual Observatory (VO) TAP queries.

Aside from the aperture and PSF photometry for the point sources, the images also contain extended sources. The optical detection of extragalactic sources beyond the MW is hampered in the ZoA, where the stellar crowding and Galactic absorption are rather extreme (see Sect. 8.3).

7. Examples of data usage: Tile e1084, Carina Nebula, and NGC 3324

7.1. Multicolour images and catalogues

One of the first images released by the JWST is of the Carina Nebula[11]. The nebula is located within the Disk to Longitude +230 area, in tile e1084, which has central coordinates RA, Dec (J2000) = 10:30:32.86, −58:39:41.8, corresponding to $l, b = -74.524725, -0.649149$ deg. The JHK_s observations of tile e1084 were carried out on March 19, 2018. Table 4 summarises the observational log. A composite false colour image combining the JHK_s images can be produced with the Aladin Sky Atlas[12] for e1084 using the WCS data in the reader of each image to determine their location, rotation and image scale.

In Fig. 7, we compare the three colour JHK_s image obtained with VISTA/VIRCAM with its JWST/NIRcam counterpart. Both images have $\sim 9 \times 7$ arcmin size, with a different orientation than equatorial or Galactic coordinates. JWST composite image comprises separate exposures containing F090W, F187N, F200W, F335M, F444W, F470N NIRCam narrow and wide filters. These filters are part of both the short and long wavelength channels, covering wavelengths from 0.901 to 4.707 microns, corresponding to pixel scales of 0.031″pixel^{-1} and 0.063″pixel^{-1} for the short and long wavelength channels, respectively. Although the JWST images were taken at a broader

[8] https://www.eso.org/rm/api/v1/public/releaseDescriptions/181
[9] http://archive.eso.org/cms.html
[10] http://vsa.roe.ac.uk/
[11] https://www.nasa.gov/image-feature/goddard/2022/nasa-s-webb-reveals-cosmic-cliffs-glittering-landscape-of-star-birth/
[12] https://aladin.cds.unistra.fr/

Table 4. Multicolour observations of tile e1084.

Band	Obs. date (2018-03-20UT)	Airmass	Exp. time (s)	Seeing (″)	ZP (mag)	Maglim (mag)	N-sources	N-flags −1	+1	−2	(sum)
H	06:35:58.7520	1.494	24.00	0.72	23.71	18.72	998,946	605,248	314,151	65,572	(98.6%)
K_s	06:41:43.4729	1.514	8.00	0.73	22.88	17.17	592,401	338,805	229,305	18,006	(98.9%)
J	06:45:19.4624	1.527	60.00	0.74	23.61	19.95	1,013,278	641,619	288,262	72,230	(98.9%)

Notes. Observational log and catalogue information for the multicolour observations of the VVVX tile e1084. All observations were labelled as 'Completed' and 'ESO Grade A'. The catalogues are dominated by stellar (−1), non-stellar (+1) and borderline stellar (−2) sources, accounting for ∼99% of the total number in each catalogue.

Fig. 7. VVVX composite image of the Carina Nebula compared with the JWST image of the same field. The VVVX image (top) is in false colour and based on the JHK_s observations while the JWST image (bottom) comprises separate exposures containing F090W, F187N, F200W, F335M, F444W and F470N NIRCam filters. The Carina Nebula is located towards tile e1084 in the Disk to Longitude +230 region of VVVX, with the JHK_s observations secured on March 19, 2018. The images have $\sim 9 \times 7$ arcmin size and are oriented with the north to the right and east to the top. Credits (JWST image): NASA, ESA, CSA, and STScI, J. DePasquale (STScI).

range of longer wavelengths (0.90–4.70 μm compared to 1.25–2.15 μm for VISTA), the VVVX images are comparable in quality for relatively bright point sources, while the nebular structure definition is clearly superior in the JWST. For faint sources, the higher resolution of JWST compared to VISTA allows the first to reach several magnitudes deeper at the same wavelengths.

Near the Carina Nebula (Fig. 7) we find NGC 3324, a stellar cluster first described by Kharchenko et al. (2005), based on PPMLX and 2MASS data. As described before VVVX offers NIR data not only with a much better resolution, but also reaches several magnitudes deeper. In Fig. 8 we present the J, H and K_s band images for the cluster. It is possible to note the difference in the gas transparency towards longer wavelengths, especially in the lower part of the images where the gas concentration is higher, increasing the number of background sources that can be observed.

We created a multicolour catalogue for tile e1084 by cross-matching the J, H and K_s band catalogues provided by CASU (aperture photometry, see Table 4). For the cross-match

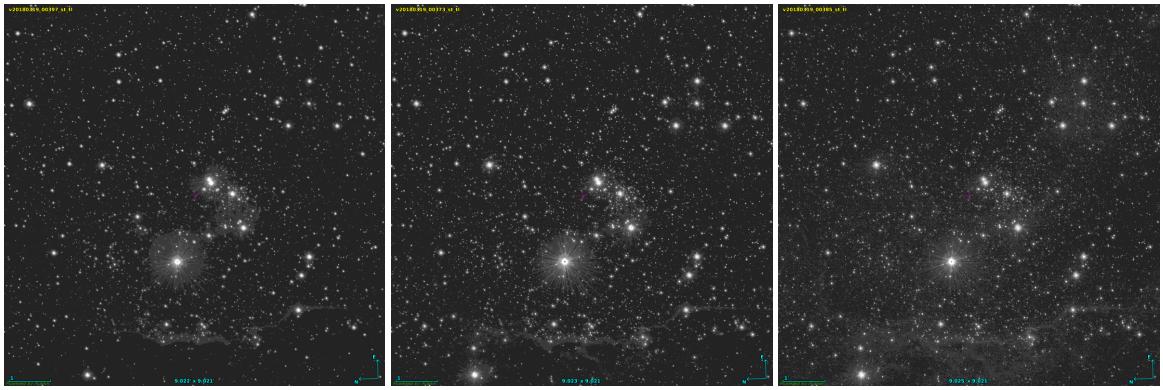

Fig. 8. Individual J (left), H (centre) and K_s band images (right) of the star cluster NGC 3324. The image is centrered at RA/DEC (J2000)=10:37:21.8, −58:36:54, with 9 arcmin side and oriented in Galactic coordinates.

procedure we made use of STILTS[13] (Taylor 2006), allowing a tolerance of 1″ between the sky coordinates of the detected sources, resulting in a JHK_s band catalogue with 568k sources, which is limited by the shorter exposure time in the K_s band compared with the other filters (see Table 2). Multiepoch K_s band images can be coadded to provide a deeper catalogue; however, that has not been applied here. In using the photometric flags and selecting only stellar sources in all 3 bands (flag '–1', see previous section), the number of sources in the e1084 catalogue dropped from 568k to 262k sources. The $J \times (J - K_s)$ CMD of stellar sources in tile e1084 is presented in Fig. 9. We have also similarly prepared CMDs for the region of Carina and NGC 3324, for the same areas presented in Figs. 7 and 8.

In order to demonstrate the importance of the PSF photometry, we also present CMDs using PSF data for the same regions mentioned above: tile e1084, the Carina Nebula region, and NGC 3324. We are currently finishing the PSF atlas for the whole VVVX area (Alonso-García et al. in prep.), building on our previous experience extracting the PSF photometry from the original VVV footprint (Alonso-García et al. 2018). A preliminary version of the PSF catalogues was used to build the CMDs of these areas of interest in Fig. 9.

Although there is excellent agreement between the aperture and PSF photometries, a larger number of sources in the PSF catalogues is evident since our algorithm to extract the PSF photometry uses a less conservative limit than the CASU aperture photometry. This difference becomes larger for the more crowded fields over the Galactic plane where the PSF is far more efficient. The VVVX PSF catalogues for the entire area will be described in Alonso-Garcia et al. (in prep.) and publicly released to the community through VSA.

7.2. Variability data: Light curves and proper motions

Dékány et al. (2013) present the effects of the time-domain sampling on the detection efficiency of variable stars. They showed that even a random cadence in the observations will allow us to detect RR Lyrae and δ-Cepheids at K_s=14 mag unambiguously, provided a minimum number of 25 epochs. Therefore, between 25–40 individual K_s band observations were allocated to the new extended survey area. More frequent observations (40 epochs) were assigned to more highly reddened regions in the new VVVX disk area at $230° < l < 295°$ (see Fig. 2), given that fainter variable stars require a larger number of observing epochs, and distant parts of the Galactic disk lie mainly in reddened, low latitude regions. Moreover, the number of epochs also depends on the type of variable star we expect to find in each region; for short-period variables, a greater number of epochs is required. Similarly, we have simulated the gain in proper motion precision of VVVX, relative to VVV. We find that 10 epochs offers the best compromise between precision and time spent, yielding an uncertainty of 300 $\mu as\,yr^{-1}$ thanks to the 9.5 yr baseline. This very high precision is essential to enable high quality decontamination of star clusters to K_s = 15–16 mag in very crowded inner Galaxy fields and our goal of 5D mapping of Galactic structure. VVVX astrometry in VIRAC2 is placed on the *Gaia* absolute astrometric reference frame, which is very precise even in the plane due to the *Gaia* method of simultaneously observing two widely separated fields.

With the long time-baseline, the high precision proper motion measurements can disentangle the bulk bulge/disk stellar motions, producing a global pure bulge/disk colour-magnitude diagram (Libralato et al. 2015). As the innermost regions of the MW bulge and central disk remain out of reach for *Gaia* observations due to their high dust extinction, it will be up to VVV and VVVX to provide input catalogues for spectroscopic surveys such as MOONS, the Milky Way Mapper (MWM; Kollmeier et al. 2017) and others.

The observing strategy for e1084 consists in 41 K_s band epochs over a baseline of 4-years, which allows the search and study of various classes of variable and transient stars, including pulsating variable stars used as distance indicators, such as RR Lyrae and Cepheids. The complete set of K_s band source catalogues for tile e1084 were matched following the same procedure as for the multicolour catalogue in order to construct the light curves for the tile. Figure 10 shows the light curves derived and subsequently phase folded for two previously known RR Lyrae stars discovered by *Gaia* in the region of tile e1084 (Rimoldini et al. 2023).

By applying a Lomb–Scargle (LS) algorithm (Lomb 1976; Scargle 1982; Zechmeister & Kürster 2009) we detected the periodic signal, albeit in the case of *Gaia* DR3 5255393833932660992 with the double period, which is a common feature in this type of analysis (e.g. Catelan et al. 2013; Ferreira Lopes et al. 2020; Botan et al. 2021). This factor-of-two error in the period determination is a well-known issue that affects the LS method (and its variants) when faced with nearly sinusoidal light curves, both in the near-IR as in the optical (e.g. Graham et al. 2013, 2017; VanderPlas 2018). In applying the string length minimisation method

[13] https://www.star.bris.ac.uk/~mbt/stilts/